

1 **How much does the snow surface influence ice crystal**
2 **concentration measurements at mountain-top stations**
3 **or**
4 **Does it make sense to measure ice crystal number concentration**
5 **at mountain-top stations?**

6 **Alexander Beck¹, Jan Henneberger¹, and Ulrike Lohmann¹**

7 ¹Institute for Atmospheric and Climate Sciences, ETH Zurich, Zurich, Switzerland

8 **Key Points:**

- 9 • In-situ measurements of microphysical cloud properties with a holographic Imager
10 • Influence of in-situ cloud observations at mountain top stations by ground based ice
11 enhancement processes
12 •

13 **Abstract**

14 In-situ cloud observations at mountain-top research station regularly measure ice crystal
 15 number concentrations (ICNCs) orders of magnitudes higher than expected from mea-
 16 surements or simulations of ice nuclei particle concentrations. Several studies suggest
 17 mountain-top in-situ measurements are influenced by surface-based ice-enhancement pro-
 18 cess, e.g. blowing snow, hoar frost or riming on snow covered trees, rocks and the remain-
 19 ing snow surface. A strong influence of in-situ observations on mountain-top stations by
 20 surface-based ice-enhancement processes may limit relevance of such measurements and
 21 could have an impact on orographic clouds.

22 This study assesses the influence of surface-based ice-enhancement processes on
 23 in-situ cloud observations at the Sonnblick Observatory in the Hohen Tauern Region,
 24 Austria. Vertical profiles of ICNCc above a snow covered surface were observed up to
 25 a height of 10 m. A decrease of the ICNC by at least a factor of two is observed, if the
 26 maximum ICNC is larger than 1001^{-1} . This decrease extended up to one order of mag-
 27 nitude during in cloud conditions and reached its maximum of more than two orders of
 28 magnitude when the station was not in cloud. ... These observations strongly suggest that
 29 mountain-top in-situ measurements poorly represent the true properties of the cloud in
 30 contact with the surface. They are influenced not only by surface-based ice-enhancement
 31 processes, but possibly also by ICNC enhancement due to turbulent layers above the sur-
 32 face.

33 **1 Introduction**

34 The microphysical properties (e.g. phase composition, cloud particle number con-
 35 centrations) and cloud processes are key parameters for the clouds lifetime, the cloud ex-
 36 tent, as well as the intensity of precipitation they produce [Rotunno and Houze, 2007]. For
 37 example, the phase composition influence the radiative properties of midlevel clouds in
 38 the temperature range between 0 to -35 °C. A pure ice cloud in this temperature regime
 39 reflects 17 W m^{-2} more radiation than an pure liquid cloud [Lohmann, 2002]. A well rep-
 40 resentation of orographic mixed-phase clouds is therefore crucial for accurate weather pre-
 41 dictions in alpine terrain and improved climate models.

42 In-situ measurements are important to improve our understanding of microphysical
 43 properties and fundamental processes of orographic mixed-phase clouds [Baumgardner
 44 et al., 2011] and are frequently conducted at mountain-top research stations. Despite an
 45 improved understanding on the origin of ice crystals from nucleation (citation!!!!) as well
 46 as from secondary ice-multiplication processes [Field et al., 2017], the source of most of
 47 the ice crystals observed at mountain-top stations and their impact on the development of
 48 the cloud remains an enigma (citation!!!!).

49 In-situ observations with aircraft usually observe ICNC on the order of $1-101^{-1}$
 50 [Gultepe et al., 2001], whereas at mountain-top research stations (e.g. Elk Mountain, USA
 51 or Jungfraujoch, Switzerland) or near the snow surface in the Arctic ICNCs of several
 52 hundreds to thousands per liter are frequently reported [Rogers and Vali, 1987; Lachlan-
 53 Cope et al., 2001; Lloyd et al., 2015]. Secondary ice multiplication processes like frag-
 54 mentation [Rangno and Hobbs, 2001] or the Hallett-Mossop process [Hallet and Mossop,
 55 1974] are usually ruled out as the source for the observed ice crystals due to the lack of
 56 large ice crystals, respectively large cloud droplets or the wrong temperature range. In-
 57 stead surface-based ice-enhancement processes are proposed to produce such enormous
 58 ICNCs. Rogers and Vali [1987] suggested two possible processes as a source for the ob-
 59 served ICNC: riming on trees, rocks and the snow surface or the lifting of snow particles
 60 from the surface, i.e. blowing snow. In addition, Lloyd et al. [2015] suggested hoar frost
 61 as a wind independent, surface-based ice-enhancement process to cause ICNCs larger than
 62 1001^{-1} for which they didn't observe a wind dependency as expected for blowing snow.

63 Although different studies are strife about the mechanisms to explain the measured high
 64 ICNCs, they agree on an strong influence by surface-based processes.

65 While the influence of mountain-top measurements by surface-based processes is
 66 widely accepted, the impact of re-suspended ice crystals on the development of super-
 67 cooled orographic clouds, e.g. a more rapid glaciation and enhanced precipitation, has not
 68 been studied extensively [Geerts *et al.*, 2015]. If the proposed surface-based ice-enhancement
 69 processes have the potential to impact the development of a cloud depends primarily on
 70 the penetration depth of the reseuspended particle into a cloud, i.e. the maximum height
 71 above the surface to which the particles get lifted.

72 The height dependency of blowing snow has been studied in the context of snow
 73 redistribution ("snow drift") and reduced visibility due to the re-suspended ice crystals
 74 by observing ice crystals up to several meters above the snow surface [Schmidt, 1982;
 75 Nishimura and Nemoto, 2005]. It has been reported that blowing snow occurs above a
 76 wind speed threshold that varies between 4 m s^{-1} and 13 m s^{-1} [Bromwich, 1988; Li and
 77 Pomeroy, 1997; Mahesh *et al.*, 2003; Déry and Yau, 1999]. Besides the wind speed, the
 78 concentration of blowing snow depends on the snowpack properties () and on the atmo-
 79 pheric conditions (current temperature, humidity) [Vionnet *et al.*, 2013]. Nishimura and
 80 Nemoto [2005] observed the ICNC up to a height of 9.6 m and found that the ICNCs usu-
 81 ally decrease to as low as 1-10 particles per liter. During a precipitation event, the relative
 82 importance of the small ice crystals below $< 100 \mu\text{m}$ decreases from nearly 100 % at 1.1 m
 83 to below 20 % at 9.6 m. The rapid decrease of ICNCs with height observed by these
 84 studies may limit the impact of blowing snow on orographic clouds. However, most of these
 85 studies were conducted in dry air conditions where ice crystals undergo rapid sublimation
 86 [Yang and Yau, 2008], which may limit the applicability of these results.

87 *Lloyd et al.* [2015] suggested that vapor grown ice crystals on the crystalline sur-
 88 face of the snow cover, i.e. hoar frost, may be detached by mechanical fracturing due to
 89 turbulence independent of wind speed. To our knowledge only one modelling study ex-
 90 exists, which asses the impact of haor frost on the development of a cloud. *Farrington et al.*
 91 [2015] implemented a flux of surface hoar crystals in the WRF (Weather Research and
 92 Forecasting) model based on a frost flower aerosol flux to simulate ICNCs measured at the
 93 Jungfraujoch by *Lloyd et al.* [2015]. They concluded, that the surface-based ice-crystals
 94 have a limiting impact on orographic clouds because the ice crystals are not advected high
 95 into the atmosphere. However, more measurements of ice-crystal fluxes from the snow
 96 covered surface are necessary to simulate the impact of surface-based ice-crystal enhance-
 97 ment processes on the development of orographic clouds [*Farrington et al.*, 2015].

98 In contrast to these finding, several remote sensing (i.e. satellite, lidar and radar)
 99 studies measured ice crystals advected as high as 1 km above the surface, which suggest
 100 an impact of surface-originated ice-crystals on clouds. Satellite observations of blow-
 101 ing snow from MODIS and CALIOP over the Antarctica [Palm *et al.*, 2011] observed
 102 layer thickness up to 1 km with an average thickness of 120 m for all observed blowing
 103 snow events. Similar observations from lidar measurements exist from the South Pole
 104 with an observed layer thickness of ice crystals of usually less than 400 m, but some rare
 105 cases when a subvisual layer exceeded a height of 1 km [Mahesh *et al.*, 2003]. However, a
 106 possible suspension of clear-sky precipitation could not be ruled out as a source of the
 107 observed ice crystal layers. Observations of layers of ice crystals from radar measure-
 108 ments on an aircraft in the vicinity of the Medicine Bow Mountains [Vali *et al.*, 2012]
 109 observed ground-layer snow clouds which where most of the time not visually detectable
 110 but produced a radar signal. Resuspended ice crystals from the surface or riming of cloud
 111 droplets at the surface can be the origin of the ice crystals in such ground-layer snow
 112 clouds. *Geerts et al.* [2015] presented evidence for ice crystals becoming lofted up to
 113 250 m in the atmosphere by boundary layer separation behind terrain crests and by hy-
 114 draulic jumps. Also evidence that ice crystals from the surface may lead to the glaciation
 115 of supercooled orographic clouds and enhanced precipitation were found. However, *Geerts*

116 *et al.* [2015] also mention the limitation of radar and lidar measurement to separate the
 117 small ice crystals produced by surface processes from the larger falling snow particles
 118 and more abundant cloud droplets. They even concluded, that "to explore BIP (blowing
 119 snow ice particle) lofting into orographic clouds, ice particle imaging devices need to be
 120 installed on a tall tower, or on a very steep mountain like the Jungfraujoch".

121 In this study we assess the influence of surface-based ice-enhancement processes
 122 on in-situ cloud observations at mountain-top stations and the a potential impact on oro-
 123 graphic mixed-phase clouds. Vertical profiles of the ICNC up to a height of 10 m above
 124 the surface were observed for the first time on a high-altitude mountain station with the
 125 holographic imager HOLIMO [Beck *et al.*, 2017]. HOLIMO is capable of imaging ice
 126 crystals larger than 25 μm and the shape of these ice crystals can be analyzed.

127 2 Field Measurements at the Sonnblick Observatory

128 2.1 Site description

129 This field campaign was conducted at the Sonnblick Observatory (SBO) situated at
 130 the summit of Mt. Sonnblick at 3106 masl (12°57'E, 47°3'N) in the Hohen Tauern Na-
 131 tional Park in the Austrian Alps. The SBO is a meteorological observatory operated all
 132 year by the ZAMG (Central Institute for Meteorology and Geodynamics). On the East and
 133 South the SBO is surrounded by large glacier fields with a moderate slope, whereas on the
 134 Northeast a steep wall of approximately 800 m descends to the valley (Fig. 1, right). Part
 135 of the SBO is a 15 m high tower used for meteorological measurements by the ZAMG.
 136 The data presented in this paper was collected during a field campaign in February 2017.

137 2.2 Instrumentation

138 The properties of hydrometeors were observed with the holographic Imager HOLIMO,
 139 which is part of the HoloGondel platform [Beck *et al.*, 2017]. The holographic Imager was
 140 mounted on an elevator that was attached to the meteorological tower of the SBO (Fig. 2)
 141 to obtain vertical profiles of the hydrometeor properties up to a height of 10 m above the
 142 surface where the platform was repeatedly positioned at five different heights as indicated
 143 in Figure 2. The holographic imager HOLIMO had a distance of approximately 1.5 m
 144 from the tower on the east-northeast side of the tower (Fig. 1, right).

145 The holographic imager HOLIMO yields single particle informations, e.g. size, and
 146 shadowgraphs from all cloud particles in a three-dimensional volume on a single image,
 147 a so-called hologram. Per hologram, a sample volume of 16 cm^3 with a length of 6 cm
 148 along the optical axis is examined. Concentrations and particle size distributions are cal-
 149 culated over 50 holograms corresponding to a volume of 800 cm^3 . The open source soft-
 150 ware HoloSuite [Fugal, 2017] is used to reconstruct the in-focus images of the particles.
 151 Particles smaller than 25 μm are classified as liquid droplets, whereas particles larger
 152 than 25 μm are separated in liquid droplets and ice crystals based on the shape of their
 153 2D image. Similar to a study by Schlenzeck and Fugal [2017] the ice crystals were further
 154 visually classified into three different groups: regular, irregular and aggregates. Because
 155 the visual classification of several thousands of ice crystals is time consuming this sub-
 156 classification of ice crystals was done only for the profiles on February 17th.

157 A single vertical profile was observed within a time interval of 10-12 min. There-
 158 fore, the holographic imager HOLIMO was positioned at an individual height for 2 min and
 159 holograms were recorded at 4 fps. This results in 81 of sampled air.

160 Meteorological data are available from the measurements by the ZAMG. The ZAMG
 161 measures one minute averages of temperature, relative humidity and horizontal wind speed
 162 and direction at the top of the meteorological tower. Snow cover depth is daily manually
 163 observed by the operators of the SBO. Based on these measurements the change of the

164 snow cover is calculated. However, this calculation includes all the changes in the snow
 165 cover depth, e.g. snow drift, sublimation, melting and fresh snow. Daily measurements of
 166 the total precipitation are available on the North and South side of the SBO. A ceilometer
 167 located in the valley on the North of the SBO measured the cloud base and cloud depth.

168 In addition, a 3D sonic anemometer was mounted at the top of the meteorological
 169 tower. However, data is only available occasionally, because most of the time the heating
 170 of the anemometer was not sufficient enough to prevent the build up of rime on the mea-
 171 surement arms.

172 3 Results

173 The data presented were observed on 4 February and 17 February 2017. Figure 3
 174 and 4 show an overview on the meteorological conditions on both days. The main differ-
 175 ence is the wind direction, which was South-West on 4 February and North on 17 Febru-
 176 ary.

177 3.1 4 February 2017

178 On 4 February a low pressure system moved eastwards from the Atlantic Ocean over
 179 northern France to western Germany, where it slowly dissipated. Influenced by this low
 180 pressure system the wind at the SBO predominantly came from West-Southwest and wind
 181 speeds between 10 and 25 m s⁻¹ (Fig. 3). In the late afternoon, around 1900 UTC, when
 182 the low pressure system dissipated over western Germany, the wind direction changed to
 183 North and wind speeds decreased to a minimum of 5 m s⁻¹. After 1900 UTC wind speed
 184 increased again to up to 15 m s⁻¹. Starting from 0800 UTC the SBO was in cloud except
 185 for a short time interval between 1910 and 2020 UTC. Because no data is available from
 186 the 3D sonic anemometer, only one minute averages are available from the ZAMG mea-
 187 surements.

188 The temperature didn't change much during the day and stayed between -10 and -
 189 9 °C until 1900 UTC when the wind direction changed to North and the temperature de-
 190 creased to -11 °C at 22 UTC.

191 Between 0830 and 2200 UTC, a total of 24 vertical profiles were obtained. Most
 192 of the profiles were obtained when the station was in cloud expect for four profiles be-
 193 tween 1910 and 2020 UTC (blue shaded in Fig. 3). The ICNC reaches a maximum at
 194 2.5 m above the surface (Fig. 5). Compared to this maximum, the mean ICNC at a height
 195 of 10 m decreases by a factor of two and the median ICNC even by a factor of four. These
 196 strong decrease of ICNC with height suggest that the majority of the ice crystals near the
 197 ground originate from the snow surface.

198 The whole measurement time period during the 4 February was divided in four pe-
 199 riods representing different conditions (Fig. 6). Between 1910 and 2010 UTC (Fig. 6
 200 third row), when the SOB was not in cloud, the ICNCs have their maximum at a height
 201 of 2.5 m. The maximum ICNC at this height reaches up to 600 l⁻¹. For three of the pro-
 202 files, the ICNC decrease by more than a factor of 5 from over 100 l⁻¹ at 2.5 m to less than
 203 20 l⁻¹ at 10 m. The mean ICNC decreases from around 100 l⁻¹ at 2.5 m to 10 l⁻¹ at 10 m
 204 (Fig. 6, right panel in the third row). The large extend of the shaded area at 2.5 m rep-
 205 presents the high variability of the ICNC even when the data is averaged over 800 cm³.
 206 Because the SBO was not in cloud during this time period, these measurements strongly
 207 suggest that up to several hundreds of ice crystals per liter originated from surface-based
 208 processes at a height of 2.5 m and at a wind speed of less than 10 m s⁻¹.

209 Between 2030 and 2200 UTC (Fig. 6 first row), when the SBO was in cloud again,
 210 the vertical profiles of the ICNC show a similar tendency as in the cloud free period. The
 211 maximum of the ICNC was observed at a height of 4.1 m and the ICNC decreases con-

212 sistantly for all four profiles with height above the observed maximum. The mean of the
 213 ICNC decreases by a factor of 9 from its maximum at 4.1 m to its minimum at 10 m. This
 214 decrease is in the same order of magnitude as in the cloud free case discussed above. As-
 215 suming that the observed ICNC at 10 m is representative for the cloud without surface
 216 influence, the surface-based processes contribute with several hundreds of ice crystals per
 217 liter to the measurements at 2.5, 4.1 and 6.0 m. This surface-based contribution is in the
 218 same order of magnitude as the total measured ICNCs in the cloud free period observed
 219 between 1910 and 2020 UTC. In contrast to the cloud free period, the surface influence
 220 extends to a height of 6.0 m, which can be explained by the increased wind speed of up to
 221 15 m s^{-1} .

222 The highest ICNCs were observed in the time period between 1200 and 1500 UTC
 223 (Fig. 6 second row) when also the wind speed reaches its maximum of 25 m s^{-1} . The box-
 224 plot shows a maximum ICNC at 2.5 m in the range of 500 to 900 l^{-1} and a decrease by a
 225 factor of 2 within 7.5 m. This decrease is much lower than observed in the previous time
 226 interval and is most likely due to the high wind speeds. Between different profiles the
 227 ICNC changed by a factor of ???, however, the trend of a decreasing ICNC with height
 228 was observed consistently for all profiles.

229 In the morning between 0830 and 1100 UTC the observed ICNCs (Fig. 6 first row)
 230 are much lower than between 1200 and 1500 UTC, although wind speed was as high as
 231 20 m s^{-1} . A possible reason is that the last snow fall was observed ??? days before the
 232 measurement. During these time, the loose ice crystal at the surface where blown away
 233 and the snowpack was solidified by temporal melting and re-freezing the snowpack [Kann
 234 man das so schreiben?]. Consequently, higher wind speeds are necessary to resuspend ice
 235 crystals from the snowpack.

236 The correlation between wind speed and ICNC on a 1 min time scale is shown in
 237 Figure 7. The maximum wind speed is used rather the average wind speed, because it is
 238 expected that the gusts, i.e. the highest wind speed in an time interval are most relevant
 239 for resuspending ice crystals from the surface. For the time interval between 0830 an 1500
 240 UTC when the wind direction was west-southwest no correlation is observed with wind
 241 speeds higher than 14 m s^{-1} (Fig 7, top). For the time interval between 1910 and 2230
 242 UTC, when the wind direction was north, a much more pronounced dependency of the
 243 ICNC on wind speed is observed for wind speeds lower than 14 m s^{-1} (Fig 7, bottom).
 244 ICNCs reached a saturation for wind speed larger than 14 m s^{-1} .

245 3.2 17 February 2017

246 On 17 February a cold front over northern Europe was moving southwards causing
 247 mainly northerly flow across the alps and at the SBO (Fig. 4). Wind speeds observed at
 248 the SBO in the time interval between 1800 and 2000 UTC were between 5 and 10 m s^{-1} .
 249 In the same time interval temperature decreased by 1 K from -12.5 to -13.5°C . The SBO
 250 was in cloud starting from 1300 UTC with varying visibility between several meters up to
 251 several hundreds of meters. Some snow fall was observed in the afternoon between 1300
 252 and 1500 UTC.

253 For this day, wind data of the 3D Sonic Anemometer are available, which allow a
 254 more detailed analysis of the correlation between the observed ICNC and wind speed. Un-
 255 fortunately, only four vertical profiles were obtained due to hardware problems with the
 256 computer. The first profile was measured in the morning at 1200 UTC when the SBO was
 257 not in cloud and no ice crystals were observed. Three more profiles were observed in the
 258 late afternoon starting from 1800 UTC. For these profiles the ice crystals have been classi-
 259 fied by hand and subclassified in the three categories: regular, irregular and aggregates.

260 The three profiles observed in the late afternoon of 17 February showed ICNCs of
 261 several hundreds in the lowest height intervals with a maximum between 4.1 and 6.0 m

(Fig. 8). The minimum ICNC was consistently observed for all profiles at 10 m and was always below 150 l^{-1} . The decrease of the ICNC with height varies between a factor of 2 and 4. In general the observed profiles on this day are similar to the ones observed on 4 February between 2030 and 2200 UTC when similar meteorological conditions were present. Wind direction was mainly from North to Northeast and wind speed varied between 5 and 10 m s^{-1} in both measurement intervals. Only temperature was slightly lower on 17 February.

In contrast to the data of 4 February, no correlation between ICNCs and the horizontal wind speed is observed (Fig. 9). This holds true for the one minute averages and maximum wind speeds observed by the SBO as well as the one second averages observed with the 3D sonic anemometer. However, an the ICNC increased with the vertical wind speed.

All the ice crystals observed on 17 February were classified by hand into aggregates, irregular and regular ice crystals (Fig. 10). ICNCs are dominated by irregular ice crystals, which is in good agreement with various other observations (citations). However, it is surprising that the relative importance of the irregular ice crystals stays constant with height or even increases (Fig. 10 right panels). Surface-based ice-crystal enhancement processes are expected to produce irregular ice crystals. With increasing height this influence is expected to decrease and regular ice crystals are expected to become more important. However, from this data a proportional decrease of the absolute number of regular and irregular ice crystals is observed. The wind dependency of the ICNC of irregular and regular ice crystals is comparable, and both increase by a factor of 2 when the vertical wind speed increased from $0\text{-}2 \text{ m s}^{-1}$ to $4\text{-}6 \text{ m s}^{-1}$ (Fig. 11). Whereas the shape of the size distribution of the irregular ice crystals does not vary much with height, larger regular ice crystals are stronger reduced than smaller regular ice crystals (Fig. 12).

4 Discussion

4.1 Comparison with the properties of blowing snow observed in the Arctic

To better understand if the observed ice crystals are resuspended particles from the surface the ice crystals shape was analyzed. The observation on 17 February were sub-classified into three different habits: regular, irregular and aggregates and the results were compared to previous studies about blowing snow. Many of these studies limited to height intervals below 2 m above the snow surface because their main focus was the redistribution of snow and its effect on road visibility, avalanche danger as well as mass and energy balance. To our knowledge only *Nishimura and Nemoto* [2005] conducted measurements of the properties of blowing snow up to a height of 9.6 m at Mizuho Station, Antarctica. However, it is important to keep in mind that also this study was conducted over a flat surface in dry air conditions.

Assumption: the majority of the irregular ice crystal comes from the ground, whereas the majority of the irregular originated in the cloud. The concentrations of ice crystals originated from the ground show a height dependency, whereas the ice crystals from the cloud do not. What would be the effects on the size distribution and sizes?

It is known that the particle size distribution at different heights can be well represented with two-parameter gamma probability density functions [*Budd*, 2013; *Schmidt*, 1982]

$$f(d) = \frac{d^{\alpha-1}}{\beta^\alpha \Gamma(\alpha)} \exp\left(-\frac{\beta}{d}\right) \quad (1)$$

with the particle diameter d , the shape parameter α and the scale parameter β . The fitted results for 17 February are shown in Figure 13 for both regular and irregular ice

309 crystals. The fits show close agreement with the data for both habits and all heights. The
 310 resulting shape parameter α and the mean diameter, represented by the product of the
 311 shape and scale parameter of the gamma-pdf, are plotted in Figure 14.

312 The mean diameter of the regular ice crystals decreases with increasing height from
 313 120 to 70 μm , whereas the mean diameter of the irregular ice crystals is constant at 100 μm .
 314 The shape factor for the irregular ice crystals also varies only little, whereas the shape fac-
 315 tor for the regular ice crystals increases from 5 to 7 at a height of 10 m. Compared to the
 316 results of ?? the parameters of the size distribution of the regular ice crystals compare
 317 much better to the properties of blowing snow than the of irregular crystals. This is puz-
 318 zling, because blowing snow has been observed to have dominantly ice crystals of irreg-
 319 ular habits (citation). For the data observed between 1910 and 2000 UTC on 4 February,
 320 which is clearly ?Why? a blowing snow event, inspection of the ice crystal habit by eye
 321 confirm these results.

322 4.2 Wind dependency of the observed ICNCs

323 The observations on 4 February and 17 February show a different correlation of the
 324 ICNC with wind speed. Whereas the ICNCs observed on 4 February show a dependency
 325 only for horizontal wind speed below 14 m s^{-1} (Fig. ???), on 17 February a correlation
 326 is only observed with vertical wind speed available from the 3D sonic anemometer (Fig.
 327 9). On 4 February, the missing wind dependency for horizontal wind speeds larger than
 328 14 m s^{-1} is probably due to a saturation of the concentration of blowing snow.

329 About reasons for the discrepancy between the two measurement days can only be
 330 speculated, because the vertical wind speed is not available for 4 February. The orography
 331 might plays an important role for the wind speed dependency. The north side of the SBO
 332 is a steep wall of 800 m. Therefore, vertical winds may transport ice crystals from this
 333 wall up to the ridge of the mountain, where they finally become lifted into the air.

334 In previous literature, a wind dependency for ICNCs smaller than 100 μm was ob-
 335 served, whereas larger ICNCs were wind independent [Lloyd *et al.*, 2015]. Blowing snow,
 336 receptively hoar frost were proposed as the underlying mechanisms for these observations.
 337 Our observations suggest that at mountain-top research station not only the horizontal
 338 wind speed play an important role for the resuspension of ice crystals, but also the ver-
 339 tical wind speed. This may be particularly true for research stations with steep orography,
 340 like the SBO and the High Altitude Research Station Jungfraujoch, Switzerland.

341 It has to be mentioned that various difficulties exist when it comes to observe the
 342 correlation between wind speed and ICNC. Firstly, ICNCs are usually compared to a si-
 343 multaneously measured wind speed. However, the observed ice crystals have been resus-
 344 pended some time before the measurement and transported in the air for a short time. In
 345 this case the simultaneously observed wind speed is not necessarily the driving force of
 346 the process of particle lifting. Secondly, wind and ICNC measurements may be performed
 347 at two different locations. Especially at mountain-top research station with its many struc-
 348 tures, local turbulence responsible for the resuspension of the observed ice crystals may be
 349 not well represented by such a wind measurement. Thirdly, the ICNC does not only de-
 350 pend on wind speed, but also on age of the snow cover and atmospheric conditions and a
 351 possible correlation may suppressed in a data set with different snowpack and atmospheric
 352 conditions.

353 4.3 Influence

354 In this case a different mechanism has to be responsible for the decrease if the ICNC
 355 of regular and irregular ice crystals observed on 17 February (Fig. 10). Possibly a turbu-
 356 lent layer above the surface enriches the ICNC of irregular as well as regular ice crystals.
 357 In this case surface-based ice-crystal enhancement processes only infrequently increase

358 the ICNC irregular crystals as observed in one profile at a height of 6 m and on 4 February
 359 2017. This also explains why a wind dependency was observed for the irregular ice
 360 crystals but not the regular ice crystals. If such an effect is responsible for the decrease of
 361 the ICNC, the differences in the size distribution of irregular and regular ice crystals can
 362 still not fully be explained. The differences between the irregular ice crystals and the ob-
 363 servations of blowing snow by *Nishimura and Nemoto* [2005] is possibly due to the miss-
 364 ing sublimation of ice crystals in cloud as it was observed in this study. This can explain
 365 the observation of a constant mean diameter with height, whereas the mean diameter in
 366 dry air decreased. An explanation of the decrease of the mean diameter of the regular ice
 367 crystals can not be given at this point and further observations are necessary to fully un-
 368 derstand the findings of this study.

369 5 Conclusion

370 This study assess the influence of mountain-top in-situ measurements by surface-
 371 based ice-crystal sources and possible implications on atmospheric relevance of such mea-
 372 surements. An elevator was attached to the meteorological tower of the SBO, Austria and
 373 vertical profiles of the ICNC were observed with the holographic imager HOLIMO on two
 374 days in February 2017. The main findings are:

- 375 • ICNCs decreases with height. ICNCs near the ground are at least a factor of two
 376 smaller than 10 m above the ground (if the ICNC near the ground is larger than
 377 100 l^{-1}). The increase in ICNCs near the ground can be up to an order of mag-
 378 nitude during cloud events and even two magnitudes during cloud free periods.
 379 In-situ measurements of the ICNC at mountain-top research stations close to the
 380 surface overestimate the ICNC by at least a factor of two.
- 381 • The ICNCs increases with increasing wind speeds up to 14 ms^{-1} by a factor of
 382 2???. Irregular ice crystals show a stronger wind dependency than regular ice crys-
 383 tals. This is agreement with the observation that surface-based ice-crystals enhance-
 384 ment processes dominantly produce irregular ice crystals.
- 385 • On 17 February a similar decrease ?What decreases? of the concentration of irreg-
 386 ular and regular ice crystals is observed, which can not be explained by surface-
 387 based ice crystal enhancement processes. Possibly turbulent layer close to the sur-
 388 face contributes to an enriched ICNC.
- 389 • The strong influence of surface-based ice-crystals sources on the measurements
 390 on mountain-top stations limits the atmospheric relevance of such measurements.
 391 However, the data set obtained is to small to make a clear statement under which
 392 conditions in-situ measurements at mountain-top research station may well repre-
 393 sent the real properties of a cloud in contact with the surface and when not.
- 394 • Further and more extensive field campaigns are necessary to better understand the
 395 mechanisms, which are responsible for the enhanced ICNC observed close to the
 396 surface at mountain-top research stations. Especially the reason for an increased
 397 concentration of irregular ice crystals near the surface is not understood. The in-
 398 fluence of the surface-based ice-crystal on the clouds could be studied more accu-
 399 rately by extending the height of the vertical profiles, e.g. by using a larger mast or
 400 a tethered balloon system.

401 Acronyms

- 402 **ICNC** Ice Crystal Number Concentration
 403 **HOLIMO** HOLographic Imager for Microscopic Objects
 404 **SBO** Sonnblick Observatory

405 **Acknowledgments**

406 Sonnblick Observatory and team (Elke Ludewig, Hermann Scheer, Norbert Daxbacher,
 407 Lug Rasser, Hias Daxbacher)

408 Thanks to Hannes, Olga, Fabiola, Monika, for their help

409 Thanks to Rob for many discussions

410 **References**

- 411 Baumgardner, D., J. Brenguier, A. Bucholtz, H. Coe, P. DeMott, T. Garrett, J. Gayet,
 412 M. Hermann, A. Heymsfield, A. Korolev, M. KrÃdmer, A. Petzold, W. Strapp,
 413 P. Pilewskie, J. Taylor, C. Twohy, M. Wendisch, W. Bachalo, and P. Chuang (2011),
 414 Airborne instruments to measure atmospheric aerosol particles, clouds and radiation:
 415 A cook's tour of mature and emerging technology, *Atmos. Res.*, 102(1â€§2), 10 – 29,
 416 doi:10.1016/j.atmosres.2011.06.021.
- 417 Beck, A., J. Henneberger, S. Schöpfer, J. Fugal, and U. Lohmann (2017), Hologondel, *At-*
 418 *mos. Meas. Tech.*
- 419 Bromwich, D. H. (1988), Snowfall in high southern latitudes, *Reviews of Geophysics*,
 420 26(1), 149–168, doi:10.1029/RG026i001p00149.
- 421 Budd, W. F. (2013), *The Drifting of Nonuniform Snow Particles1*, pp. 59–70, American
 422 Geophysical Union, doi:10.1029/AR009p0059.
- 423 Déry, S. J., and M. K. Yau (1999), A climatology of adverse winter-type weather
 424 events, *Journal of Geophysical Research: Atmospheres*, 104(D14), 16,657–16,672, doi:
 425 10.1029/1999JD900158.
- 426 Farrington, R. J., P. J. Connolly, G. Lloyd, K. N. Bower, M. J. Flynn, M. W. Gallagher,
 427 P. R. Field, C. Dearden, and T. W. Choularton (2015), Comparing model and measured
 428 ice crystal concentrations in orographic clouds during the inupiaq campaign, *Atmos.*
Chem. and Phys., 15(18), 25,647–25,694, doi:10.5194/acpd-15-25647-2015.
- 429 Field, P. R., R. P. Lawson, P. R. A. Brown, G. Lloyd, C. Westbrook, D. Moisseev, A. Mil-
 430 tenberger, A. Nenes, A. Blyth, T. Choularton, P. Connolly, J. Buehl, J. Crosier, Z. Cui,
 431 C. Dearden, P. DeMott, A. Flossmann, A. Heymsfield, Y. Huang, H. Kalesse, Z. A.
 432 Kanji, A. Korolev, A. Kirchgaessner, S. Lasher-Trapp, T. Leisner, G. McFarquhar,
 433 V. Phillips, J. Stith, and S. Sullivan (2017), Secondary ice production: Current state of
 434 the science and recommendations for the future, *Meteorological Monographs*, 58, 7.1–
 435 7.20, doi:10.1175/AMSMONOGRAPH-D-16-0014.1.
- 436 Fugal, J. P. (2017), Holosuite, in preparation.
- 437 Geerts, B., B. Pokharel, and D. a. R. Kristovich (2015), Blowing Snow as a Natural
 438 Glaciogenic Cloud Seeding Mechanism, *Mon. Weather Rev.*, 143(12), 5017–5033, doi:
 439 10.1175/MWR-D-15-0241.1.
- 440 Gultepe, I., G. Isaac, and S. Cober (2001), Ice crystal number concentration versus tem-
 441 perature for climate studies, *International Journal of Climatology*, 21(10), 1281–1302,
 442 doi:10.1002/joc.642.
- 443 Hallet, J., and S. Mossop (1974), Production of secondary ice particles during the riming
 444 process, *Nature*, 249, 26–28, doi:10.1038/249026a0.
- 445 Lachlan-Cope, T., R. Ladkin, J. Turner, and P. Davison (2001), Observations of cloud and
 446 precipitation particles on the avery plateau, antarctic peninsula, *Antarctic Science*, 13(3),
 447 339â€§348, doi:10.1017/S0954102001000475.
- 448 Li, L., and J. W. Pomeroy (1997), Estimates of threshold wind speeds for snow trans-
 449 port using meteorological data, *Journal of Applied Meteorology*, 36(3), 205–213, doi:
 450 10.1175/1520-0450(1997)036<0205:EOTWSF>2.0.CO;2.
- 451 Lloyd, G., T. W. Choularton, K. N. Bower, M. W. Gallagher, P. J. Connolly, M. Flynn,
 452 R. Farrington, J. Crosier, O. Schlenczek, J. Fugal, and J. Henneberger (2015), The ori-
 453 gins of ice crystals measured in mixed-phase clouds at the high-alpine site jungfraujoch,
 454 *Atmos. Chem. Phys.*, 15(22), 12,953–12,969, doi:10.5194/acp-15-12953-2015.

- 456 Lohmann, U. (2002), Possible aerosol effects on ice clouds via contact nucleation, *Journal of the Atmospheric Sciences*, 59(3), 647–656, doi:10.1175/1520-
457 0469(2001)059<0647:PAEOIC>2.0.CO;2.
- 458 Mahesh, A., R. Eager, J. R. Campbell, and J. D. Spinhirne (2003), Observations of blowing snow at the south pole, *Journal of Geophysical Research: Atmospheres*, 108(D22),
459 n/a–n/a, doi:10.1029/2002JD003327, 4707.
- 460 Nishimura, K., and M. Nemoto (2005), Blowing snow at mizuho station, antarctica, *Philosophical Transactions of the Royal Society of London A: Mathematical, Physical and Engineering Sciences*, 363(1832), 1647–1662, doi:10.1098/rsta.2005.1599.
- 461 Palm, S. P., Y. Yang, J. D. Spinhirne, and A. Marshak (2011), Satellite remote sensing of
462 blowing snow properties over antarctica, *Journal of Geophysical Research: Atmospheres*,
463 116(D16), n/a–n/a, doi:10.1029/2011JD015828, d16123.
- 464 Rangno, A. L., and P. V. Hobbs (2001), Ice particles in stratiform clouds in the arctic and
465 possible mechanisms for the production of high ice concentrations, *Journal of Geophysical Research: Atmospheres*, 106(D14), 15,065–15,075, doi:10.1029/2000JD900286.
- 466 Rogers, D. C., and G. Vali (1987), Ice crystal production by mountain surfaces, *J. Clim. Appl. Meteorol.*, 26(9), 1152–1168, doi:10.1175/1520-
467 0450(1987)026<1152:ICPBMS>2.0.CO;2.
- 468 Rotunno, R., and R. A. Houze (2007), Lessons on orographic precipitation from the
469 mesoscale alpine programme, *Quarterly Journal of the Royal Meteorological Society*,
470 133(625), 811–830, doi:10.1002/qj.67.
- 471 Schlenzeck, O., and J. Fugal (2017), Microphysical properties of ice crystal precipitation
472 and surface-generated ice crystals in a high alpine environment in switzerland, *esult*, 56,
473 433–453, doi:10.1175/JAMC-D-16-0060.1.
- 474 Schmidt, R. A. (1982), Vertical profiles of wind speed, snow concentration, and
475 humidity in blowing snow, *Boundary-Layer Meteorology*, 23(2), 223–246, doi:
476 10.1007/BF00123299.
- 477 Vali, G., D. Leon, and J. R. Snider (2012), Ground-layer snow clouds, *Quarterly Journal
478 of the Royal Meteorological Society*, 138(667), 1507–1525, doi:10.1002/qj.1882.
- 479 Vionnet, V., G. Guyomarcâžh, F. N. Bouvet, E. Martin, Y. Durand, H. Bellot, C. Bel,
480 and P. Pugliažse (2013), Occurrence of blowing snow events at an alpine site over a
481 10-year period: Observations and modelling, *Advances in Water Resources*, 55, 53 – 63,
482 doi:<http://doi.org/10.1016/j.advwatres.2012.05.004>, snowâšAtmosphere Interactions
483 and Hydrological Consequences.
- 484 Yang, J., and M. K. Yau (2008), A new triple-moment blowing snow model, *Boundary-
485 Layer Meteorology*, 126(1), 137–155, doi:10.1007/s10546-007-9215-49.

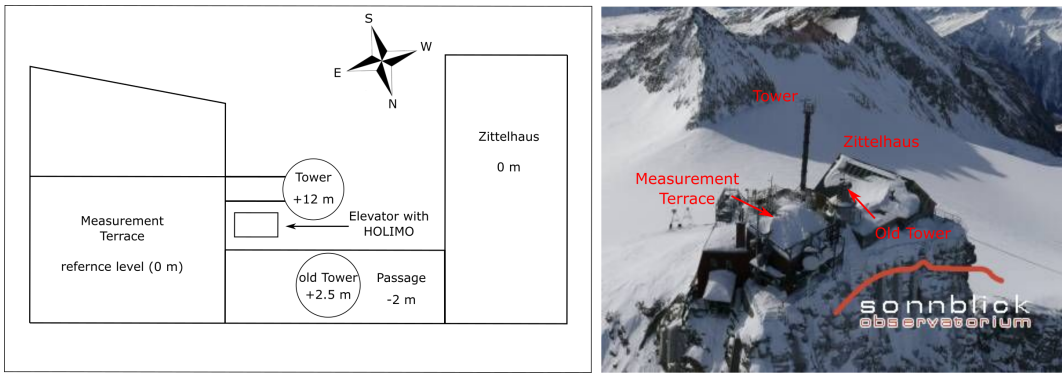


Figure 1. Sketch of the experimental setup and the surrounding structures (left) with their heights relative to the bottom of the measurement terrace. Aerial image of the Sonnblick Observatory (right).

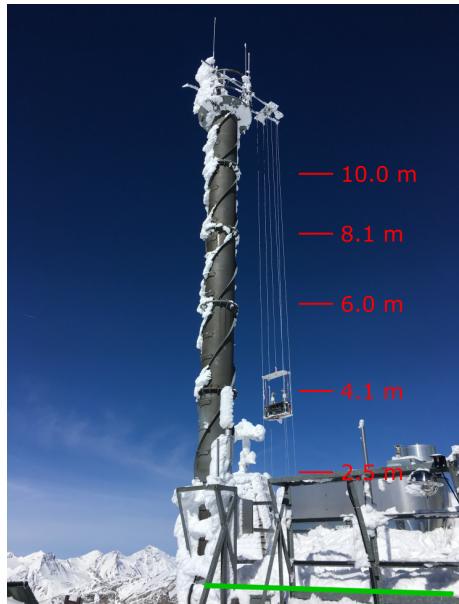
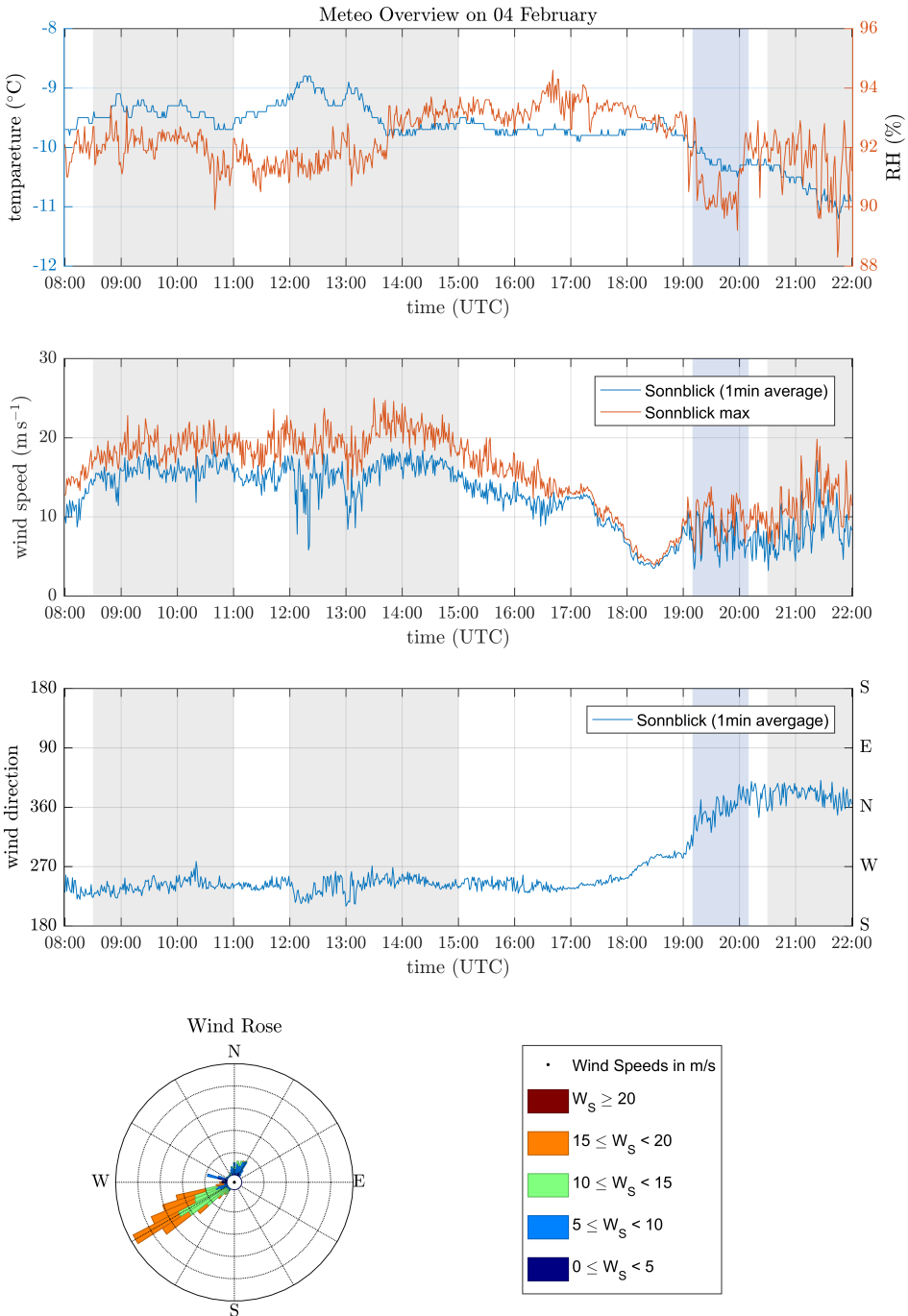
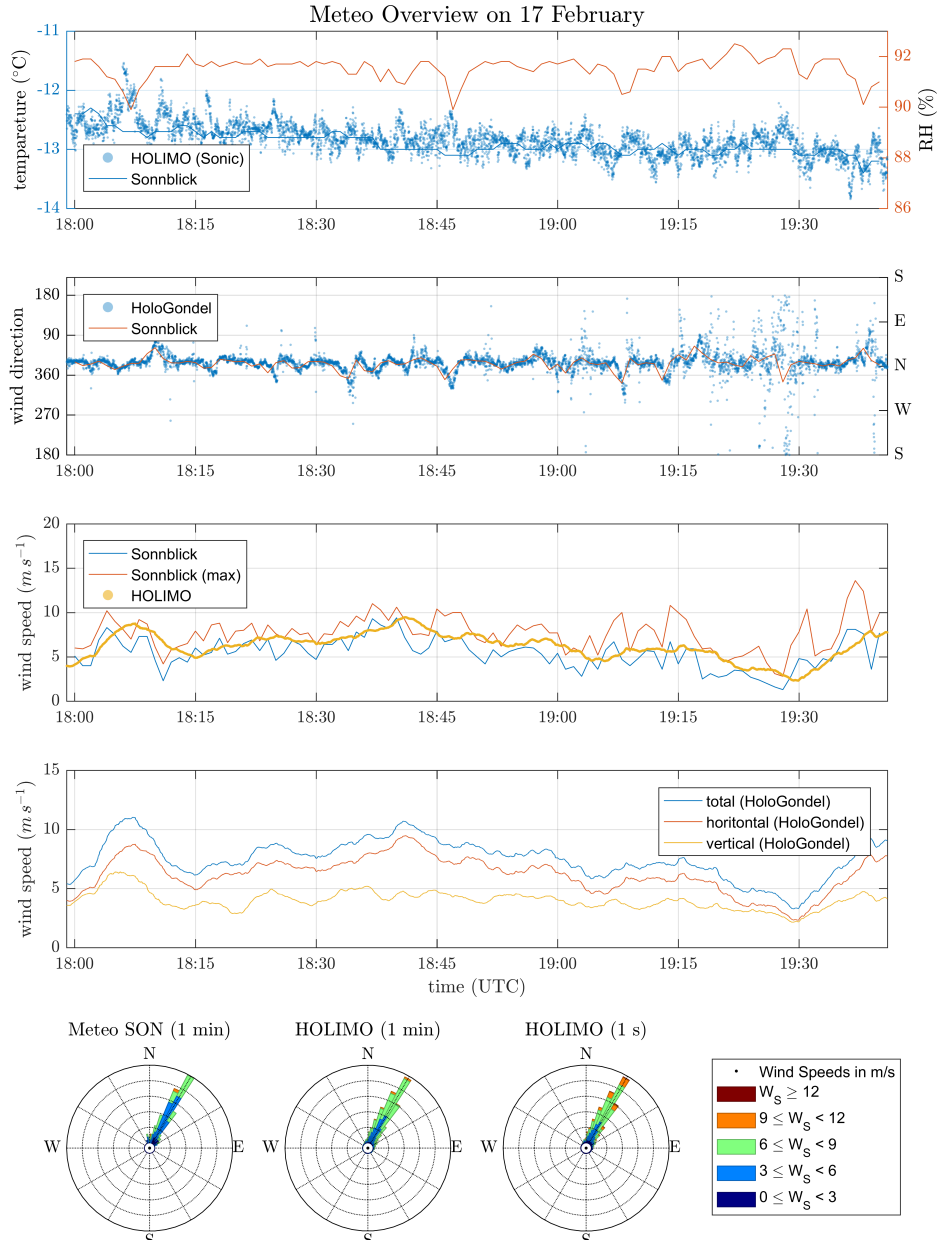


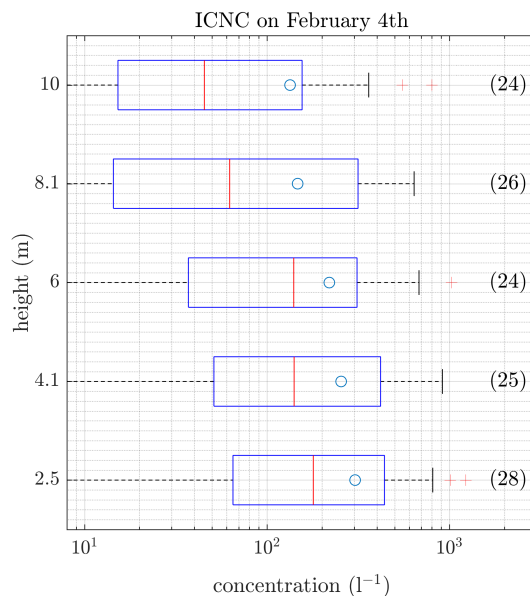
Figure 2. Set up of the elevator with the holographic imager HOLIMO mounted to the meteorological tower at the SBO. The red lines and numbers indicate the five different heights where the elevator was positioned repeatedly to obtain vertical profiles of the ICNC. The reference height of 0.0 m is the bottom of the measurement platform (green line).



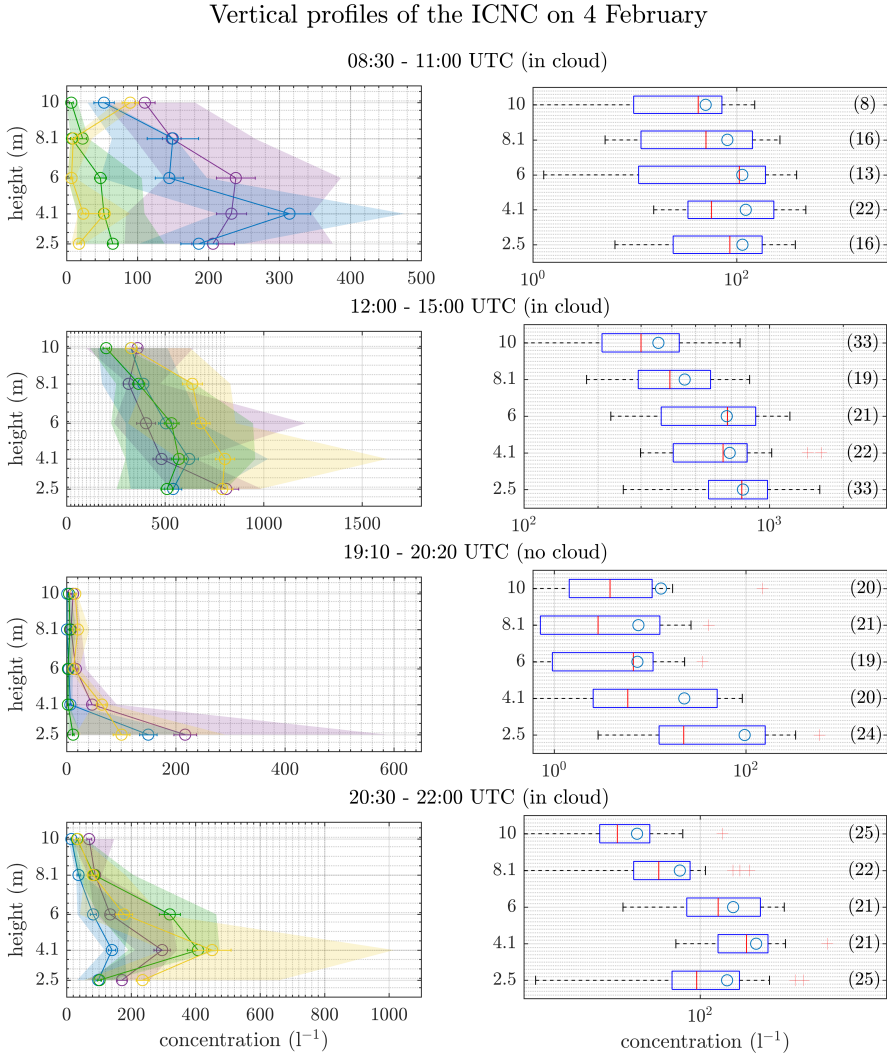
498 **Figure 3.** Overview of the meteorological conditions on 4 February obtained from the SBO measurements.
499 Shown are the temperature, relative humidity (top), wind speed (second from top) and wind direction (second
500 from bottom). All measurements are 1 min averages except for the maximum wind speed, which corresponds
501 to the maximum wind speed observed during a corresponding 1 min average. Grey and blue shaded areas
502 represent time with measurement (see Fig. 6) when the SBO was in cloud, respectively not in cloud. A wind
503 rose plot (bottom) of the wind measurement is also shown.



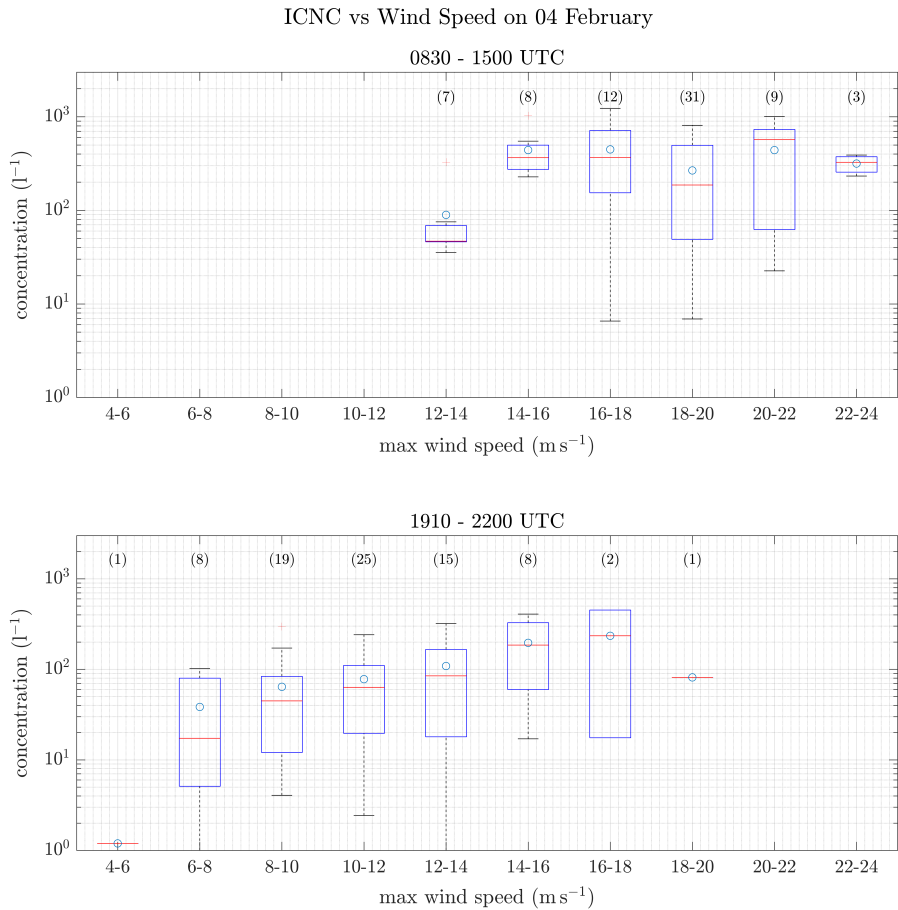
504 **Figure 4.** Overview on the meteorological conditions on 17 February for the time interval when measure-
 505 ments exist (see Fig. 8). On this day temperature and wind measurements are available from the SBO and the
 506 3D Sonic Anemometer. Shown are the temperature and relative humidity (top), wind direction (second from
 507 top), a comparison of the horizontal wind speed (middle) and detailed wind speed measurements from the 3D
 508 Sonic Anemometer (second from bottom). A windrose plot is shown in the bottom panel.



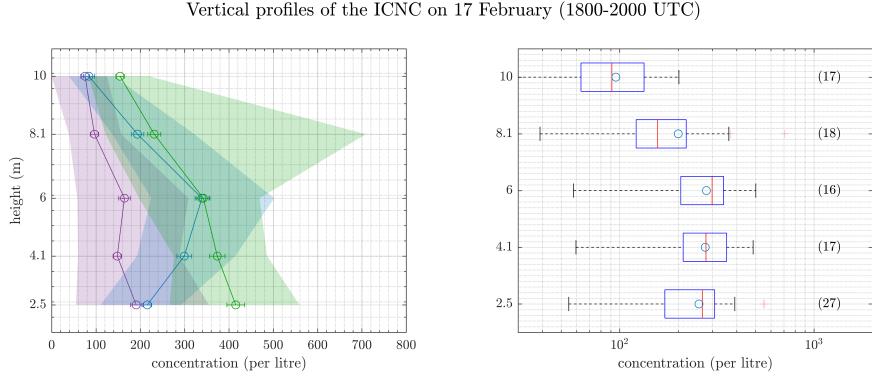
509 **Figure 5.** ICNC as a function of the height of the elevator at the meteorological tower of the SBO. This plot
 510 is a summary of the 24 profiles obtained on 4 February. The data was averaged over the entire time period
 511 of single measurements at the different height. The number in brackets is the number of concentration
 512 measurements per height. For each box, the central line marks the median value of the measurement and the
 513 left and right edges of the box represent 25th and the 75th percentiles respectively. The whiskers extend to
 514 minimum and maximum of the data; outliers are marked as red pluses. The mean value of the measurements
 515 is indicated as a blue circle.



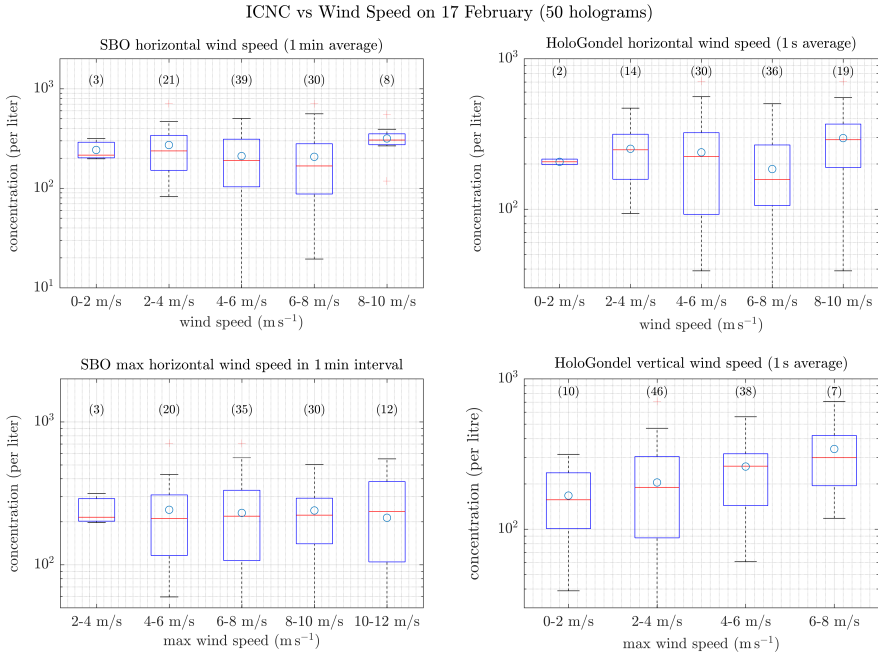
516 **Figure 6.** ICNCs as a function of height of the elevator for four different time intervals during 4 February,
517 representing different conditions (Fig. 3). On the individual profiles (left), the circles indicate the mean value
518 averaged over the entire time interval. The error bars represent the standard error of the mean. The shaded
519 area extends from the minimum to the maximum of the measured ICNC. As in Fig. 5 only for the four time
520 intervals the box plots (right) show a summary of the data.



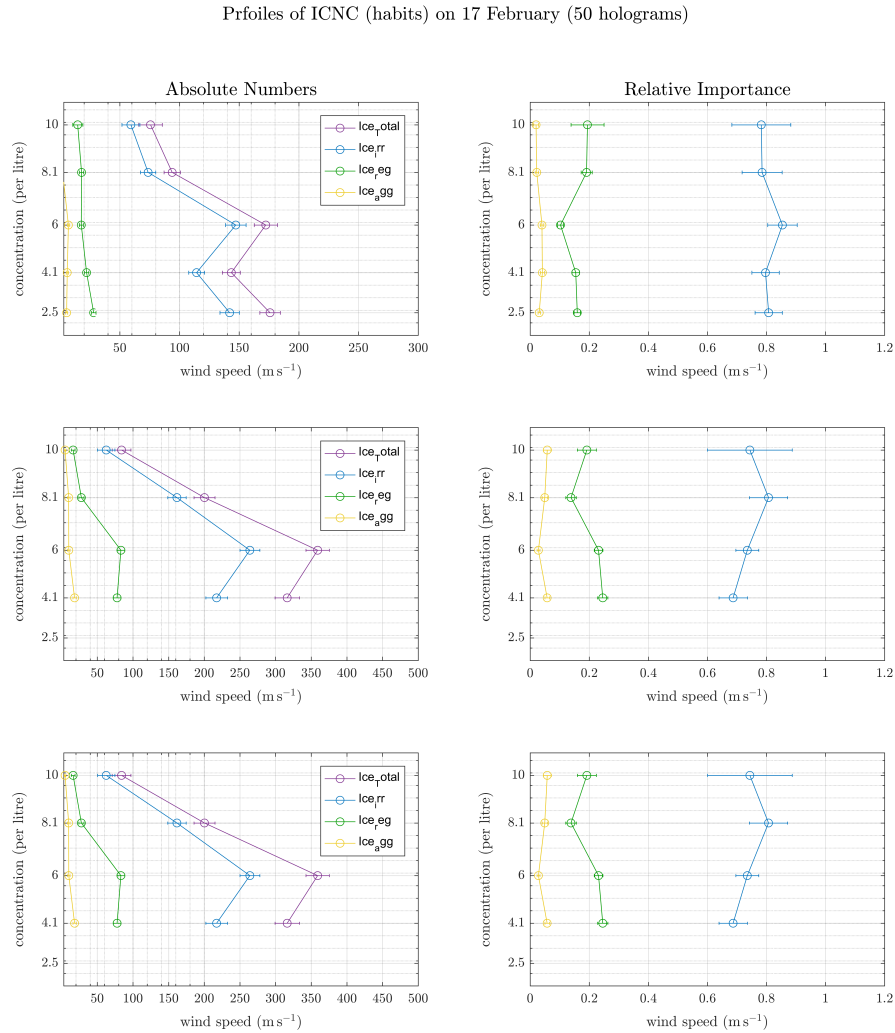
521 **Figure 7.** As Figure 5 only ICNC as a function of horizontal wind speed for the the time periods between
 522 0830 and 1500 UTC when the wind direction was West-Southwest (top) and between 1910 and 2200 UTC
 523 when the wind direction was North (bottom). The wind speed is the maximum wind speed in one minute time
 524 intervals from the SBO.



525 **Figure 8.** Ice crystal number concentration as a function of the height of the elevator at the meteorological
 526 tower of the SBO for 17 February. On the left are the three individual profiles obtained in cloud. The circles
 527 indicate the mean value averaged over the entire time interval. The error bars represent the standard error of
 528 the mean. The shaded area indicates the variability of the data and extends from the minimum to the maxi-
 529 mum when the data is averaged over 50 holograms. For the summary of the different time intervals (right) the
 530 data is averaged over 50 holograms. For each box, the central line marks the median value of the measurement
 531 and the left and right edges of the box represent 25th and the 75th percentiles respectively. The whiskers
 532 extend to minimum and maximum of the data; outliers are marked as red pluses.



533 **Figure 9.** As Figure 7 only for 17 February and four different wind speed measurements: a) one minute
 534 averages of the horizontal wind speed from the SBO, b) maximum wind speed of the a corresponding time
 535 interval in a), c) secondly averages of the horizontal wind speed and d) secondly average of the vertical wind
 536 speed both from the 3D Sonic Anemometer.



537 **Figure 10.** Vertical profiles of the concentration (left) and the relative importance (right) of the subclassified
 538 ice crystal habits: regular, irregular and aggregates. For the relative importance the number of ice crystals
 539 of different habits were divided by the total number of ice crystals. For theses plots the data as averaged
 540 over 50 holograms. In both cases the circles represent the mean of the 50 hologram averages. The error bars
 541 represent the standard error of the mean.

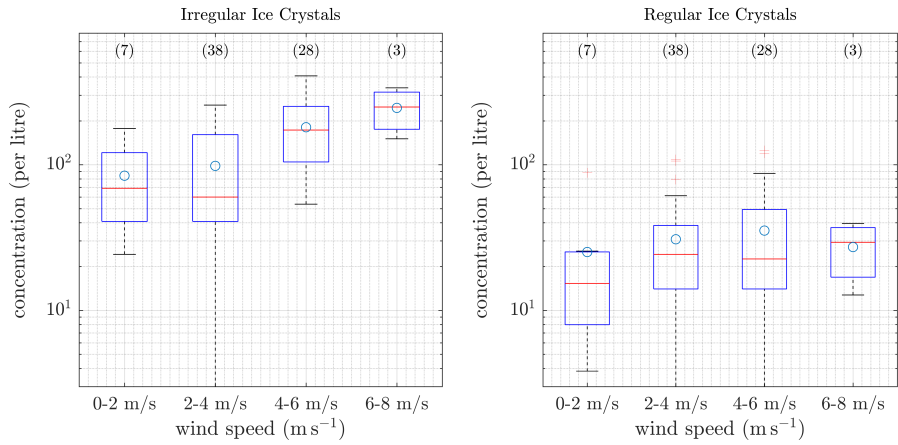


Figure 11. As Figure 7 only for 17 February and the ICNC of different ice crystal habits as a function of the vertical wind speed.

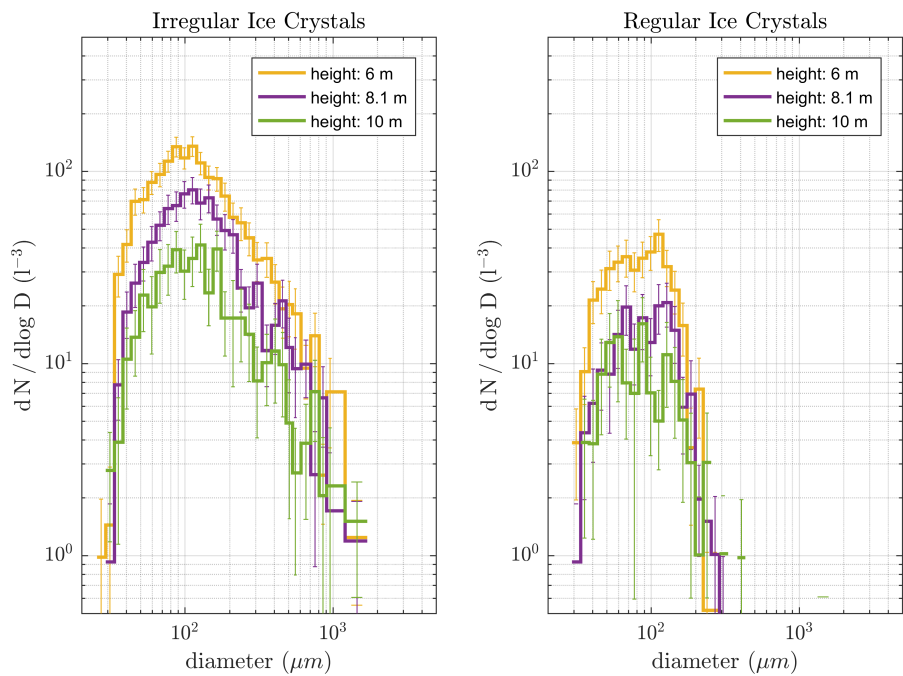
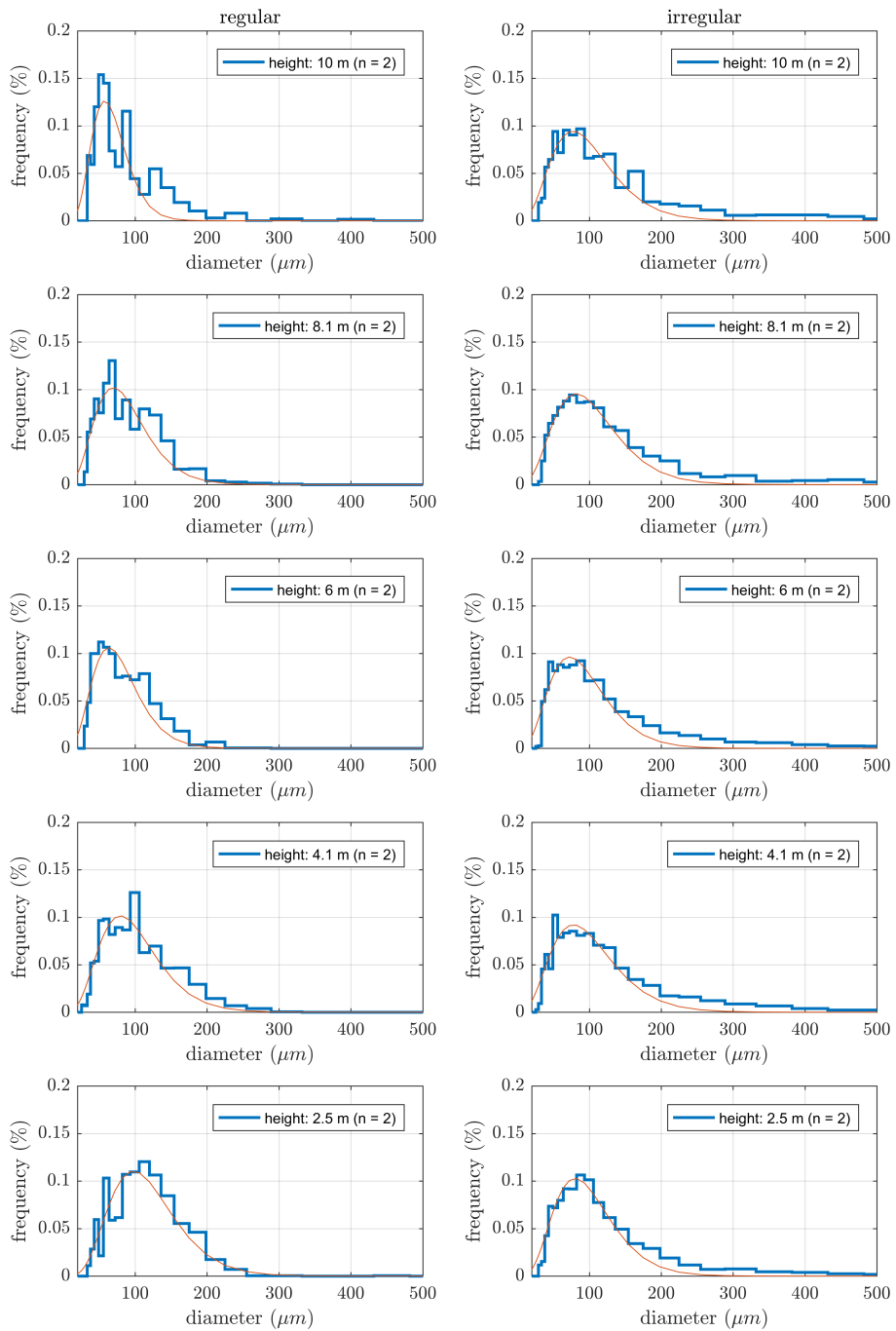
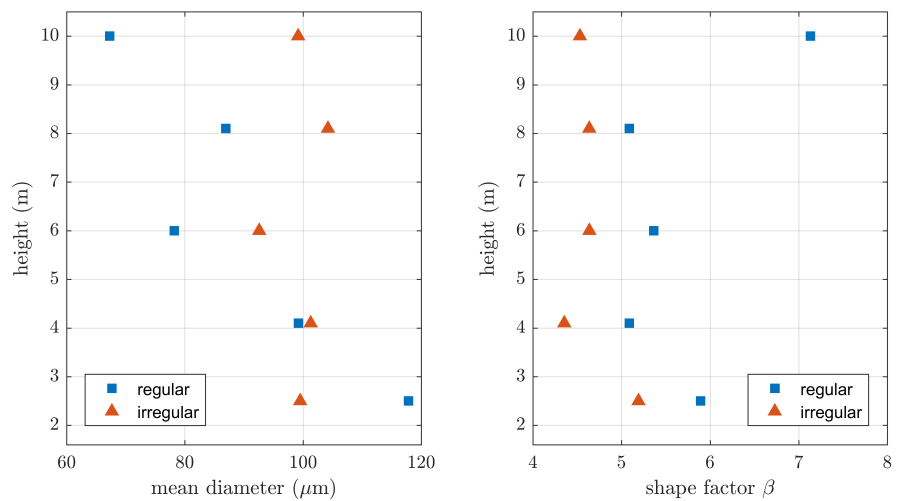


Figure 12. Size distribution of the irregular (left) and regular (right) ice crystals observed on 17 February as a function of height. The errorbars represent the standard error of the mean.



546 **Figure 13.** Probability distribution of the particle diameter for regular (left)
 547 and irregular (right) ice crystals
 548 measured on 17 February. The red line indicates the result of the fit of the two parameter gamma-pdf from
 equation (1).



549 **Figure 14.** Profiles of the mean diameter (left) and the shape parameter (right)
550 of the two parameter gamma-pdf (Eq. (1)) plotted as a function of height.